

Effects of histone methyltransferase inhibition in endometriosis

Running title: Histone methylation in endometriosis

Summary sentence: Inhibition of the histone methyltransferase EZH2 reduced H3K27me3 levels in the endometriotic cells specifically, and also reduced their migration, proliferation but not their invasion.

Keywords: Endometriosis, Endometrium, Epigenetics, Histone modifications

Authors and affiliations:

Mariano Colón-Caraballo, PhD¹; Annelyn Torres-Reverón, PhD²; John Lee Soto-Vargas³; Steven Young, MD/PhD⁴, Bruce Lessey, MD/PhD⁴, Adalberto Mendoza, MD^{5,6}, Raúl Urrutia, MD⁷, and Idhaliz Flores, PhD^{1,8}

¹Department of Basic Sciences-Microbiology Division, Ponce Health Sciences University, Ponce, Puerto Rico

²Department of Biomedical Sciences, Division of Neurosciences, University of Texas at Rio Grande Valley-School of Medicine, Texas, USA

³Department of Basic Sciences-Microbiology Division, Step-Up Summer Program, Ponce, Puerto Rico

⁴Department of Ob/Gyn, University of North Carolina, Chapel Hill, USA

⁵Southern Pathology Inc., Ponce, Puerto Rico

⁶Department of Basic Sciences- Pathology Division, Ponce Health Sciences University, Ponce, Puerto Rico

⁷Epigenetics & Chromatin Dynamics Research Program, Mayo Clinic, Rochester, Minnesota, USA

⁸Department of Ob/Gyn, Ponce, Puerto Rico

Grant support

We acknowledge the funding by NIH (R01-HD050559) to IF from the National Institute for Child Health and Human Development; and RISE fellowship to MCC (R25-GM082406) from National Institute for General Medical Sciences. MCC was also supported by the American Physiological Society (APS) Porter Fellowship and by the PHSU Biomedical Sciences PhD Program (Ponce Medical School Foundation). ATR was supported by NIH K07AT008027. Construction of the Tissue Microarray (TMA) used for this study was funded by the U56 PSM-MCC Partnership (U56-CA126379) from the National Cancer Institute (NCI). Funding for collection of primary human cells was obtained from the Eunice Kennedy Shriver National Institute for Child Health and Disease, NIH (R01HD067721 to SLY. and BAL)

Conference presentation

Presented in part at the 12th World Congress on Endometriosis (WCE) 2014, Brazil, and in the 2016 Meeting of the Society for Reproductive Investigation (SRI), Canada.

Correspondence

Idhaliz Flores, PhD

Professor of Basic Sciences-Microbiology and Obstetrics-Gynecology

Director, Endometriosis Research Laboratory

Ponce Health Sciences University - School of Medicine and Ponce Research Institute

395 Calle Luis F. Salas

Ponce, Puerto Rico 00716-2348

United States

Email: iflores@psm.edu

P: (787) 840-2575 x 2006, 2192

Abstract

Although the histone methyltransferase EZH2 and its product H3K27me3 are well studied in cancer, little is known about their role and potential as therapeutic targets in endometriosis. We have previously reported that endometriotic lesions are characterized by global enrichment of H3K27me3. Therefore, we aimed to 1) characterize the expression levels of EZH2 in endometriotic tissues, 2) assess H3K27me3 enrichment in candidate genes promoter regions, and 3) determine if pharmacological inhibition of EZH2 impacts migration, proliferation, and invasion of endometriotic cells. Immunohistochemistry (IHC) of an endometriosis-focused tissue microarray (TMA) was used to assess the EZH2 protein levels in tissues. Chromatin Immunoprecipitation (ChIP)-qPCR was conducted to assess enrichment of H3K27me3 in candidate gene promoter regions in tissues. Immunofluorescence (IF) was performed to assess the effect of an EZH2-specific pharmacologic inhibitor on H3K27me3 global enrichment in cells lines. To measure effects of the inhibitor in migration, proliferation, and invasion *in vitro* we used Scratch, BrdU, and Matrigel assays, respectively. Endometriotic lesions had significantly higher EZH2 α nuclear immunostaining levels compared to eutopic endometrium from patients (glands, stroma) and controls (glands). H3K27me3 was enriched within promoter regions of candidate genes in some but not all of the endometriotic lesions. Inhibition of EZH2 reduced H3K27me3 levels in the endometriotic cells specifically, and also reduced migration, proliferation but not invasion of endometriotic epithelial cells (12Z). These findings support future pre-clinical studies to determine *in vivo* efficacy of EZH2 inhibitors as promising non-hormonal treatments for endometriosis, still an incurable gynecological disease.

Introduction

Endometriosis, an estrogen-dependent and progesterone-resistant gynecological disease, is characterized by the presence of functional endometrial-like tissue (e.g., glands and stroma) outside the uterine cavity [1]. The main clinical manifestations of women with endometriosis include dysmenorrhea, dyspareunia, chronic pelvic pain, and often infertility, which negatively impact their quality of life (QoL) [2, 3]. Several theories have been proposed to explain how endometriosis develops [4], which would require the activation of cellular processes related to survival, adhesion, invasion, and angiogenesis [5]. Epigenetics provide a unifying theory that can integrate the diversity of evidence regarding the etiology of endometriosis, via its capacity to modulate expression of selected genes (reviewed in [6]). By triggering multiple cellular behaviors commonly observed in endometriosis, epigenetic mechanisms have been proposed as attractive targets for the development of potential non-hormonal approaches for the treatment of this gynecological condition.

Histone methylation is one of the key epigenetic modifications that play a role in distinct cellular processes via modulation of the chromatin structure and transcriptional activity [7]. This mechanism is known to work alone or in combination with DNA methylation to influence gene transcription and thus determine the cellular phenotype [8]. We and others have previously shown that endometriotic lesions are characterized by hypermethylation of H3K4, H3K9, and H3K27 [9], and by high positive nuclei immunostaining of tri-methylated H3K27 or H3K27me3 [10, 11]. Recently, it has been demonstrated that “epidrugs” that target DNA methylation and histone deacetylation [e.g., DNA methyltransferases (DNMT’s) and histone deacetylases (HDAC’s), respectively] block cellular processes and behaviors characteristic of endometriosis [12-16]. However, due to non-target genomic effects and side effects seen in clinical studies for cancer, such therapies may not be considered as safe and

specific therapeutic options for endometriosis [17]. Other epigenetic mechanisms such as histone methylation/demethylation are gaining increased attention as they could represent safer options since they specifically inhibit histone methyltransferases (HMT's) or histone demethylases (HDM's) that have highly exclusive gene targets [18-20].

EZH2, the catalytic subunit of the polycomb repressive complex 2 (PCR2), is the HMT responsible for setting the addition of three methyl groups (me3) to H3K27, a repressive histone mark, via a S-adenosyl-methionine (SAM) direct mechanism [21]. Thus, the mechanism of action of EZH2 can be inhibited by SAM competitive inhibitors such as the recently discovered pyridine-indazole scaffold molecule, GSK343 [22]. Pharmacological evidence demonstrated that GSK343 is highly selective against EZH2 compared to other HMTs [22]. The best evidence for the efficacy and effects of treatment with GSK343 derives from the cancer research field. *In vitro* and *in vivo* studies have shown that this HMT inhibitor (HMTi) significantly decreases the invasive, proliferative and angiogenic capacities of cancer cells, and increases the expression of pro-apoptotic related genes [23, 24]. In addition, GSK343 induced autophagy and increased drug sensitivity [25]. Importantly, treatment of cancer cells with GSK343 was shown to change only 2% of the transcriptome [26], preferentially regulating a subset of genes involved in immune response and inflammation, in a cancer-specific manner [27]. This suggests that treatment with GSK343 will not cause substantial side effects since it does not lead to broad, unspecific changes in gene expression, although this needs to be experimentally tested.

The present study was designed to i) elucidate the expression profile of EZH2 in endometriotic and control tissues, and ii) unravel the molecular and cellular mechanisms related to the setting of

H3K27me3 in endometriosis by assessing the *in vitro* effects of GSK343, a specific inhibitor of EZH2. These studies are of great translational value given that EZH2 inhibitors are drugs that are now in Phase I/II clinical trials for cancer, and they could potentially fill the void in non-hormonal therapeutic alternatives for the treatment of endometriosis, still an enigmatic and incapacitating disease.

Materials and Methods

Ethics

Protocols involving tissue collection were approved by the PHSU-PRI, UNC-Chapel Hill, and Greenville Health System SC IRB Committees. Participants who donated fresh tissue for research signed a consent form and completed a demographical and clinical survey. Formalin-fixed paraffin-embedded blocks used for construction of the TMA were obtained in a de-identified fashion under an IRB approved protocol.

Immunohistochemistry of Human Endometrial and Endometriotic Samples on a Tissue Microarray (TMA)

A total of 164 formalin-fixed, paraffin-embedded endometrium and endometriotic tissues were used to construct a TMA at Moffitt Cancer Center, Tampa, FL. All the biopsies were evaluated by a pathologist to confirm the diagnosis of endometriosis. The total number of cores in the TMA were 34 peritoneal endometriosis, 29 ovarian endometriosis, 16 fallopian endometriosis, 7 gastrointestinal (GI) endometriosis, 4 skin endometriosis, 38 secretory phase endometria, 16 control proliferative phase endometrium, 20 control secretory phase endometrium, and 34 eutopic endometrium of women with endometriosis (14 in proliferative phase and 20 in secretory phase). Control endometria were obtained

from patients with benign gynecological conditions different to endometriosis. Immunostaining of EZH2 was conducted following standard protocols. Briefly, 10µm sections of the TMA block were cut for immunostaining. After paraffin removal and dehydration, antigen unmasking was performed. Peroxidase blocking was conducted and the TMA was incubated with the primary antibody to EZH2 alpha isoform (1:50) (kindly donated by Dr. Raúl Urrutia) at 4°C overnight, followed by incubation with streptavidin-labeled secondary antibody following the manufacturer's protocol (DAKO, Carpinteria, California). Prior to IHC, the specificity of the primary antibody as well as the working dilution were tested in neuroblastoma tissue samples. As a negative control, we used normal pre-immune control IgG as primary antibody (Alpha Diagnostics, San Antonio, TX) to evaluate non-specific staining in the tissue samples. For staining and counterstaining of the TMA, DAB and hematoxylin (Fischer Scientific, Waltham, Massachusetts) were used, respectively. The stained TMA slide was mounted and visualized at 20, 40, and 100x magnification on an inverted microscope with an Olympus 35 mm camera (Nikon, Japan). EZH2 immunostaining intensity analysis of the selected areas (e.g., glands and stroma) was performed by three independent scorers using an intensity scale (2=strong, 1=weak, and 0=no staining) in a blinded fashion [28, 29].

Tissue Collection

Fresh tissues (endometriotic lesions [n =13] and eutopic endometrium from healthy controls [n=12]) were obtained during surgery and immediately frozen at -80°C after collection. Cases were defined as women with surgically diagnosed endometriosis and healthy controls were obtained from women without any gynecologic conditions (kindly provided by Dr. Steven Young, University of North Carolina-Chapel Hill and Dr. Bruce Lessey, Greenville Health System, Greenville South Carolina). Disease severity was determined by collaborating gynecologists using the revised American

Fertility Society (rAFS). The tissues were analyzed by histopathology to confirm endometriosis, defined as the presence of endometrial glands and stroma, and to date the menstrual cycle phase according to Noyes [19]. Demographic profiles of endometriotic lesions and endometrial samples for Chromatin Immunoprecipitation (ChIP) experiments in the study are summarized in **Table 1**.

Tissue Chromatin Immunoprecipitation (ChIP) - Quantitative PCR (qPCR).

ChIP assays were conducted using the Chroma Flash High-Sensitivity ChIP Kit (Epigentek, New York, NY) following standard protocols. Briefly, the endometriotic lesions (n=13) and endometrial samples (n=12) were weighted and minced into small fragments using a scalpel. Tissues were cross-linked with 1% formaldehyde followed by incubation with 1.25M glycine and homogenized using the Bullet Blender Homogenizer. The disaggregated tissue pellet was then re-suspended in ChIP Buffer followed by sonication to shear the DNA. Samples were incubated overnight at 4°C with anti-H3K27me3 (Epigentek, NY, NY) (1ug/well) and non-immune IgG (1ug/well) antibodies, previously cross-linked to a 96-well strip. Immune-complexes and input DNA controls were incubated with RNase A at 42°C for 30 minutes followed by incubation with proteinase K at 60°C for 45 minutes for reversal of the cross-linking reaction. Finally, the samples were incubated with DNA binding solution (DBS) at 95°C for 15 minutes followed by a wash with 90% ethanol and DNA Enhancer Elution Buffer (DEB) to elute the purified DNA.

Primers specific for the promoter regions of candidate genes for endometriosis, selected based on their well-established dysregulation in this condition [6, 30], were designed using Primer 3 (v.0.4.0) software followed by promoter sequence analysis using the BLAST/NCBI program of GenBank (**Table 2**). Promoter sequences were selected based on bioinformatic analysis of histone enrichment (H3K27me3) using University of California Santa Cruz (UCSC) Genome Browser (www.genome.ucsc.edu). H3K27me3 enrichment at promoter regions were determined by ChIP-qPCR with SYBR Green Master Mix (Bio-Rad, Hercules, California) using the Real Plex iCycler System (Eppendorf, Hauppauge, NY). The amplification parameters were empirically determined for each primer pair, followed by a melt curve analysis using the Real Plex default setting. Relative fold enrichment was calculated relative to IgG using the $2^{-\Delta Ct}$ method. Experiments were conducted in triplicate.

Human Endometrial and Endometriotic Cell Cultures and Drug Treatments

The human endometrial cells (HESC), human non-endometriotic epithelial cells EEC [recently shown by DNA fingerprinting to be related to the breast cancer epithelial cell line MCF-7 [31]], and human endometriotic epithelial cells (12Z) (gifts from Dr. A. Fazleabas and Dr. A. Starzinski, respectively) were used for the experiments described herein [20]. The HESC cells were cultured in phenol-red free Dulbecco's modified Eagle's medium (DMEM) supplemented with 10% FBS Charcoal Dextran (steroid hormone depleted FCS), HEPES 1%, 1% ITS (insulin, transferrin, selenious acid), puromycin (500ng/mL) and 1% antibiotic/antimycotic. The EEC/MCF-7 cells were cultured in Dulbecco Modified Eagle Medium (DMEM/F12) Nutrient Mixture supplemented with 10% fetal bovine serum (FBS), 1% antibiotic/ antimycotic, 160 ng/mL of bovine insulin. The 12Z cells were grown in DMEM/F12 with phenol red complete media supplemented with 10% FBS, 1% antibiotic/ antimycotic, and 1% of

sodium pyruvate. Cells were maintained at 37°C in humidified incubator and 5% CO₂. Cells were treated with either GSK343 (Sigma Aldrich, St. Louis, MO) or DMSO (0.1%) as a control vehicle for the downstream assays described below.

Immunofluorescence Staining

The enrichment levels of H3K27me3 in the endometriotic and non-endometriotic cell lines were determined by immunofluorescence (IF). Briefly, treatment either with GSK343 (1µM, 10 µM, and 20 µM), 0.1% DMSO (vehicle control) or media only (basal or referent) was performed for 24 hrs and 48 hrs. Cells were fixed with 4% paraformaldehyde (PFA) at 4°C overnight followed by permeabilization with 0.5% Triton-X 100 in PBS and further incubation with blocking buffer (fresh-filtered 2%BSA in PBS). Then, the cells were incubated with primary antibody to H3K27me3 (1:1600) (Cell Signaling C36B11 Cat No. 9733) followed by incubation with Alexa Fluor 555 goat-anti rabbit IgG secondary antibody (2mg/mL) (Life Technologies Cat No. A21428). For counterstaining, the cells were incubated with DAPI (NucBlue Fixed Cell Stain Ready Probe Reagent for Light Technologies Cat No. R37606). As a negative control, cells were incubated with PBS (instead of primary antibody) and treated under the same experimental conditions as previously described. Images were acquired with Evos Immunofluorescence microscope (Life Technologies, Carlsbad, CA) using two different excitation filters: RFP (530nm excitation, 593nm emission) for Alexa-Fluor555 conjugated secondary antibody and DAPI (360nm excitation, 447nm emission) for DAPI reagent. Nuclear H3K27me3 fluorescence intensity was quantified using Image J software (NIH). Three images per well were taken immediately after staining using the same excitation parameters and illumination, and uploaded into Image J for analysis of integrated density and area of each cell. To calculate the H3K27me3 intensity, we used the corrected total cell fluorescence (CTCF) formula: $CTCF = \text{cell integrated density} - (\text{area of the cell} \times$

mean background density) as previously described [32]. The average of eight regions lacking labeling in each image was used as background. This formula compensates for background staining and variation in the level of illumination between the analyzed images. This analysis was done in three different experiments in duplicate.

In vitro Cell Migration Assay (Scratch Assay)

The migration capacity of HESC, EEC, and 12Z cells were assessed by Scratch Assay. The cells were seeded (1.25×10^5 cells) and cultured in 12 well plates until they reached ~75-80% of confluence. A scratch was performed in the middle of the well using a 100 μ l sterile pipette tip. The migration capacity of cells was measured in the presence of GSK343 (Sigma Aldrich, St. Louis, MO) at two different doses (1 μ M and 10 μ M) or 0.1% DMSO (control vehicle). Photos (20X) were taken at different time-points (0, 24, 48, and 72hrs) after the initial scratch was made using the EVOS FL microscope (Cat No. 6500-FL, Life Technologies, Carlsbad, CA) with an adapted Sony ICX445 CCD camera (1.3 megapixels). Measurement of the open wound area was conducted using automated image analysis software (T-Scratch, CSE Lab, Zurich, Switzerland) that measured the area occupied by the cells in the image [33]. Experiments were conducted three times in duplicate.

In vitro Cell Proliferation Assay

Cell proliferation rates of the cells were measured using the BrdU cell proliferation ELISA assay kit (Cat. No 2750, Millipore, Billerica, MA) according the manufacturer's protocol. Briefly, cell suspensions (1×10^4 cells in 100 μ L) were added to the wells of a 96-flatbottom microplate in appropriate serum-deprived medium in three technical replicates (3 wells). The proliferation capacity

of the cells was assessed in the presence of GSK343 (Sigma Aldrich, St. Louis, MO) at two different concentrations (10 μ M and 20 μ M) or 0.1% DMSO (control vehicle) for 24 and 48 hrs at 37°C. Spectrophotometry detection (optical density, OD) was performed at 450nm single wavelength using the BioTek Synergy HT Multimode microplate reader (BioTek, Winooski, VT). Experiments were conducted three times in triplicate.

Matrigel Cell Invasion Assay

Cell invasion was measured using BioCoat Matrigel Invasion Chambers (Cat No. 354480, Corning, Bedford, MA) following manufacturer's instructions. Briefly, cell suspensions [5 x10⁴ cells 500 μ L of serum deprived media (1% FBS)] was added to the chambers. The invasion capacity of the cells was assessed in the presence of GSK343 at 20 μ M for 24 hrs vs. 0.1% DMSO (control vehicle). Cells were fixed and stained using Diff-Quick Kit (Cat No. B4132-1A, Allegiance) as described by the manufacturer. The cells were visualized and photographed using the High Intensity LED Light Inverted Nikon Eclipse TS2R-FL microscope at 20X objective (Nikon, Melville, NY) with an adapted camera DS-Ri2 (16.25 megapixel, color, high resolution). Invasion was reported as the mean count of cells invading through the Matrigel. Two technical replicates were conducted in three independent experiments.

Statistical Analysis

Data were analyzed using GraphPad Prism version 6.0 (GraphPad Software, San Diego, California). The mean \pm SEM was used to determine differences among the groups. For EZH2 immunostaining analysis, non-parametric statistical analysis of variance (ANOVA-Kruskal-Wallis Test) followed by Dunn Multiple Comparison post-hoc test was conducted. For CHIP-qPCR analysis, Fisher's

exact test was conducted. For H3K27me3 intensity basal enrichment levels, a non-parametric Kruskal-Wallis test was conducted followed by a Dunn's multiple comparisons test. For changes in H3K27me3 intensity after GSK343 treatment, data were analyzed using a Two-way ANOVA (non-parametric and non-repeated measures because for the experiment we used two independent plates for each time point) followed by a Tukey's multiple comparisons test. In this analysis, the drug concentration (CV, 1 μ M, 10 μ M, and 20 μ M) and time (24 hrs and 48 hrs) were defined as the variables. For *in vitro* migration, non-parametric repeated Two-way ANOVA was conducted followed by a Tukey's multiple comparison test. In this analysis, the drug concentration (CV, 1 μ M, 10 μ M) and time (24 hours, 48hours, and 72hrs) were defined as variables. The data obtained from the TScratch Program was reported as percent (%) of open wound area, and transformed using $y = \sqrt{y}$ before statistical analyses. The proliferation capacity of the cells was assessed using Non-repeated measures Two-way ANOVA followed by a Tukey's multiple comparisons test. To determine statistical significance of differences in the number of cells invading the Matrigel, we used a Wilcoxon test to compare treatment with 20 μ M of GSK343 vs. CV. Statistical significance was set at $p < 0.05$.

Results

EZH2 α is Differentially Expressed in Endometriotic and Endometrial Tissues

The nuclear immunostaining intensity of EZH2 α was analyzed by immunohistochemistry in both glands and stroma of lesions and endometria from patients and controls using an endometriosis-focused TMA. No significant differences in EZH2 α immunostaining intensity were observed among lesion types in either glands or stroma. However, a significantly higher intensity staining for EZH2 α was observed in the glandular compartment of secretory endometrium from patients (1.00 ± 0.21) compared to proliferative endometrium from patients (0.04 ± 0.04) ($p < 0.05$) (**Figure 1**). Next, because

no differences between lesions were observed, we grouped all lesions to compare EZH2 α nuclear staining against endometrial samples (**Figure 2**). We observed a significantly higher intensity of EZH2 α immunostaining in the glands of the endometriotic lesions (1.68 ± 0.09) compared to both proliferative endometrium from patients (0.04 ± 0.04 , $p < 0.0001$) and controls (0.72 ± 0.25 , $p < 0.05$), and to secretory endometrium from controls (0.72 ± 0.19 , $p < 0.05$). In the stromal compartment, we detected higher EZH2 α nuclear intensity in the endometriotic lesions (1.65 ± 0.09 , $p < 0.05$) compared to proliferative endometrium from patients (0.61 ± 0.31 , $p < 0.05$). In sum, our findings clearly suggest that there is a loss of EZH2 expression in endometrium from patients and a gain of EZH2 expression in the endometriotic lesions.

Promoter Regions of Endometriosis Candidate Genes are Differentially Enriched with H3K27me3

Using ChIP-qPCR, we observed a differential enrichment of H3K27me3 at promoter regions of candidate genes when comparing endometriotic lesions and endometrial samples from healthy controls. We observed two different groups based on the level of H3K27me3 enrichment at the promoter regions using 10-fold or more enrichment as the threshold (**Table 3**). *ESR1* was the gene with highest level of H3K27me3 enrichment (69%, 9/13), followed by *CDH1* (46%, 6/13), and *PGR* (31%, 4/13). Interestingly, Fisher exact test showed that in cases (endometriotic lesions) the promoter regions of *ESR1* and *CDH1* genes have significantly ($p < 0.05$) higher H3K27me3 enrichment compared to healthy controls. These genes have been previously reported to be downregulated in lesions [34-36]. *SF-1*, on the other hand, has been reported to be elevated in endometriosis [37], and in this study 77% (10/13) of the lesions presented a < 10 -fold H3K27me3 enrichment in its promoter region. Taken together, these results demonstrate that H3K27me3 may be involved in regulating the expression of these endometriosis candidate genes in some, but not all, endometriotic lesions.

Pharmacological Inhibition of EZH2 Decreases the H3K27me3 Enrichment only in Endometriotic Cells

Nuclear levels of H3K27me3 in cell lines were determined by Immunofluorescence (IF), and data reported as CTCF (corrected total cell fluorescence) (**Figure 3**). At 24hrs, H3K27me3 enrichment levels were significantly different among the cell lines tested. Moreover, the endometriotic epithelial cells (12Z) had significantly higher basal enrichment of H3K27me3 compared only to the non-endometriotic epithelial cell line (EEC) (6374 ± 724.80 vs. 1607 ± 184.10 , $p < 0.0001$). At 48 hrs, basal enrichment of H3K27me3 in 12Z cells remained high, but not significantly different compared to the other cell lines tested.

Next, we measured the effects of pharmacological inhibition of EZH2 on the enrichment levels of H3K27me3. Cells were treated with vehicle (CV) or GSK343 ($1\mu\text{M}$, $10\mu\text{M}$, or $20\mu\text{M}$) for 24 hrs and 48 hrs. We observed that treatment of the endometriotic epithelial cells (12Z) with GSK343 at $10\mu\text{M}$ for 48hrs significantly reduced H3K27me3 levels compared to CV (1913.33 ± 392.55 vs. 4677.34 ± 1167.83 , $p < 0.05$). Treatment of 12Z cells with GSK343 at $20\mu\text{M}$ reduced H3K27me3 levels compared to CV at both 24 hrs (3182.69 ± 541.56 vs. 5935.99 ± 538.09 , $p < 0.05$) and 48 hrs (1926.23 ± 352.61 vs. 4677.34 ± 1167.83 , $p < 0.05$) (**Figure 4**). However, GSK343 did not significantly reduce the levels of H3K27me3 in the other two cell lines tested (HESC, EEC) (**Figure 5, 6**). Collectively, these results demonstrate that GSK343 modulates the enrichment levels of H3K27me3 in a specific manner affecting only the endometriotic cells. These findings suggest that this therapeutic option may not have substantial and undesired side effects, although *in vivo* experiments would need to be conducted to confirm this hypothesis.

Pharmacological Inhibition of EZH2 Impacts Cell Proliferation and Migration but not Invasion of Endometriotic Cells

The role of EZH2 inhibition on the migratory, proliferative, and invasive behaviors of the endometriotic and non-endometriotic cells was assessed using different *in vitro* assays. First, to determine the effect of EZH2 inhibition on the migratory capacity of the cells, we used Scratch assays (**Figure 7**). Across the board, 12Z cells exhibited a robust migratory capacity (low % of open wound area) compared to its counterparts. Interestingly, we found that treatment with 10 μ M GSK343 reduced the migration capacity of 12Z cells compared to CV (43.67 \pm 9.02 vs. 22.55 \pm 4.68 at 48hrs, $p < 0.05$; 36.51 \pm 3.14 vs. 8.74 \pm 2.60 at 72hrs, $p < 0.001$). For HESC cells, we also observed that 10 μ M GSK343 decreased the migration capacity of the cells compared to CV at both 48hrs (24.86 \pm 5.57 vs. 8.58 \pm 2.57, $p < 0.001$) and 72 hrs (1.63 \pm 0.91 vs. 11.84 \pm 3.32, $p < 0.001$), although the highest effect on migration was seen at 48hrs. GSK343 treatment did not modulate the migratory capacity of the EEC cells. In sum, these findings indicate that the drug impacts the migration capacity of the HESC and 12Z cells; however, the effect seems to be higher particularly in the endometriotic cells (12Z).

Next, we elucidated the effect of EZH2 inhibition on the proliferative capacity of the cells by conducting BrdU assays (**Figure 8**). We observed that treatment with GSK343 significantly diminished the proliferation capacity of the 12Z cells compared to CV [24hrs: 20 μ M (0.32 \pm 0.03) vs. CV (0.41 \pm 0.02), $p < 0.05$; 48hrs: 10 μ M (0.45 \pm 0.01) vs. CV (0.71 \pm 0.05), $p < 0.001$; and 20 μ M (0.42 \pm 0.02) vs. CV (0.71 \pm 0.05) $p < 0.0001$]. At 24hrs, a borderline significance of decreased proliferation was observed at 10 μ M compared to CV (0.33 \pm 0.03 vs. 0.41 \pm 0.02, $p = 0.053$). GSK343 treatment did not have any impact in the proliferative capacity of HESC cells, but decreased the proliferation capacity of EEC cells

at 24hrs [10 μ M (0.53 \pm 0.02) vs. CV (0.88 \pm 0.03) p <0.0001 and 20 μ M (0.43 \pm 0.01) vs. CV (0.88 \pm 0.03) p <0.0001] and at 48hrs [10 μ M (0.87 \pm 0.03) vs. CV (1.09 \pm 0.09) p <0.01 and 20 μ M (0.70 \pm 0.04) vs. CV (1.09 \pm 0.09) p <0.0001]. Together, these results suggest that EZH2 may exert an epigenetic control over the cell cycle regulatory process in endometriosis.

Ultimately, to assess the impact of EZH2 inhibition on the invasive capacity of the cell lines, we used Matrigel assays (**Figure 9**). In these experiments, we measured the inhibitory effects of GSK343 at 20 μ M on the invasion rates of the cells at 24hrs. 12Z cells had the highest capacity to invade through the extracellular matrix (ECM), but treatment did not modulate their invasiveness [20 μ M (167.5 \pm 7.41) vs. CV (154.5 \pm 8.82) p =0.2188]. However, GSK343 treatment decreased the number of HESC [20 μ M (24.05 \pm 3.95) vs. CV (33.65 \pm 4.83), p <0.05] and EEC [20 μ M (3.4 \pm 0.82) vs. CV (7.80 \pm 0.90) p <0.05] cells invading through the Matrigel. Representative pictures of Matrigel inserts (CV vs 20 μ M) are shown for visual representation. Collectively, these data demonstrate that 12Z cells are highly invasive compared to its counterparts; however, the 20 μ M GSK343 dose in particular was not effective in blocking the invasive behavior of the endometriotic cells.

Discussion

The present study was designed to add knowledge to the current evidence supporting a role of the EZH2, and its product, trimethylated H3K27, in endometriosis. First, we elucidated the expression profile of EZH2 in endometriotic lesions and endometria from patients and controls. IHC on an endometriosis TMA was done using an antibody specific for EZH2 α , one of the two known variants of the EZH2 locus that result from alternative splicing [38]. We show here that endometriotic lesions have

significantly higher EZH2 α nuclear immunostaining compared to endometria, which correlates with our previous findings of increased levels of H3K27me3 in lesions [10]. In strong support of our findings, two recent studies have reported high levels of EZH2 and H3K27me3 staining in lesions compared to endometrium from controls [11, 39]. Taken together, our results and parallel findings from an independent laboratory provide strong evidence of a higher expression of EZH2 in endometriotic tissues. Whether this aberrant expression has biological effects on endometriotic cells specifically was studied next *in vitro*.

Pharmacological inhibition of EZH2 by the histone methyltransferase inhibitor GSK343 has been recognized as a targeted approach to deplete H3K27me3 levels, thus re-setting expression signatures of selected genes in cancer cells [27]. We therefore aimed to assess the inhibiting effect of GSK343 and its specificity for endometriosis. First, we characterized the H3K27me3 basal enrichment levels *in vitro* and observed that the endometriotic epithelial cells 12Z were enriched in H3K27me3 compared to control cell lines, reflecting the high levels of expression of EZH2. Next, we showed that pharmacological inhibition of EZH2 using GSK343 reduced global H3K27me3 levels only in the endometriotic cells. Our findings are in accord with previous studies showing that GSK343 treatment (1 μ M-20 μ M) reduces the nuclear enrichment of H3K27me3 in ovarian, cervical, and prostate cancer cells leading to changes in global transcriptomic signatures [22-25]. It also reflects the observation in breast cancer cells that pharmacological blockage of EZH2 is specific to diseased cells, leaving normal cells unaffected [27].

Increased expression of EZH2 in endometriotic lesions is expected to lead to H3K27me3 enrichment at the promoter regions of candidate genes. It has been previously reported that there is

aberrant expression of *ESR1*, *PGR*, *HOXA10*, *CDH1*, and *SF-1* in endometriosis lesions, which has been linked to altered hormonal responses, impaired uterine receptivity, and activation of EMT [40]. The present study uncovers the histone methylation status—for H3K27me3 in particular—at promoter regions of these candidate genes. We observed that a high proportion of lesions were enriched in H3K27me3 at the promoter region of *ESR1*, *CDH1* and *PGR*. These results indicate that these genes can be regulated by DNA methylation and histone methylation concomitantly. It is worth noting that like DNA methylation, histone methylation does not appear to be a widespread phenomenon, since it is not seen in all the lesions studied [41]. Whether these epigenetic mechanisms are temporally regulated (i.e., present in early lesions, but lost in response to lifetime exposures including previous treatments), or due to the natural heterogeneity of endometriotic tissues will require follow up studies with larger sample sizes obtained from a broad range of patients.

High levels of EZH2, resulting in a H3K27me3 hypermethylation state, have been found to be involved in regulation of cancer-related cellular behaviors (e.g., migration, proliferation, invasion, resistance to apoptosis, angiogenesis) [42-49]. We showed here that GSK343 reduced the proliferative capacity of the endometriotic cells but also of the other epithelial cell line studied, suggesting a cell-type specific effect of this drug. In cancer, it has been demonstrated that CDKIs are downregulated by H3K27me3 [50-52] and that pharmacological inhibition of EZH2 reconstituted their normal expression followed by a concomitant decrease in cell proliferation [53-55]. Treatment with GSK343 also reduced the migration capacity of the endometriotic cells; although to a lesser extent, the endometrial stromal cells were also responsive to treatment. Notably, both cells are highly migratory and both were specifically targeted by the drug. Finally, while we observed that the endometriotic cells invaded more through the Matrigel compared to control cells, pharmacological inhibition of EZH2 did not reduce

their invasiveness. It is possible that higher doses or longer treatment times would be required to see an effect, or combination treatment with DMT inhibitors might be necessary to re-express the silenced genes involved in regulation of invasion in endometriotic cells. Future studies can be directed towards elucidating the role of EZH2 on invasion and whether combinatorial treatments would be more effective. There is already recent evidence for a role of EZH2 in inducing EMT and fibrosis in endometriotic lesions, and blocking EZH2 was shown to reduce migration and invasion of endometriotic cells *in vitro*, which adds to our current knowledge on the pathways that are relevant for this disease [39]. It would also be important to assess the effects of HMTi in other key cellular behaviors such as apoptosis, angiogenesis, and immune/inflammatory responses.

Moving forward to the potential application of HMT inhibitors for endometriosis, it is critical to assess the effects of these drugs on the eutopic endometrium of the patients. Our immunostaining experiments show an apparent “loss” of EZH2 expression in endometrium from patients vs. a “gain” in the endometriotic lesions. While additional studies are required to understand these findings, we speculate that the chronic inflammatory environment in the peritoneum of women with endometriosis could result in increased levels of EZH2 within ectopic endometrium, as shown before in other inflammatory conditions [56]. EZH2 function has been shown to be regulated by estrogen receptor signaling, and these responses may be differentially activated in ectopic vs. eutopic endometrium based on their pattern of expression of the cognate estrogen receptors [57]. Thus, additional studies are necessary to understand the physiological impact of EZH2 blockage not only in the lesions but also the endometrium.

In sum, this study demonstrated aberrant expression of EZH2 and enrichment of H3K27me3 in candidate genes for endometriosis. Moreover, we demonstrated that pharmacological inhibition of EZH2 by GSK343, a HMT inhibitor already in clinical trials for cancer, decreased H3K27me3 levels in a specific manner, while reducing the proliferative and migratory capacity of the endometriotic cells. These data from our group and others support the notion that EZH2 may be an effective therapeutic target since blocking this enzyme can impact several of the underlying cellular behaviors activated in endometriosis; however, it is important to rule out any global and undesirable effects that may be activated by blocking this epigenetic mechanism in other tissues such as the eutopic endometrium. Therefore, these findings strongly support subsequent pre-clinical studies to determine the *in vivo* efficacy and safety of EZH2 inhibitors as promising non-hormonal therapeutic options for women with endometriosis, a disease notorious from being refractory to current treatments.

Acknowledgments

The authors acknowledge the administrative of the Endometriosis Research Program Staff (Martha Báez), and the PHSU-MBRS RISE Program (Jean Marie Schmidt). We also thank Dr. Janice B. Monteiro for support in primer design and analysis of promoter regions and Dr. Abigail Ruiz for guidance during the design of the tissue culture experiments. We acknowledge the role of Dr. Miosotis García in the selection and pathological analysis of samples used in the development of the endometriosis TMA and Dr. Adalberto Mendoza, Southern Pathology Laboratories, Inc. for access to the paraffin blocks. We are grateful to OB/Gyns who collaborated with tissue accrual. Special thanks to the women who donated their tissues and data for this research.

References

1. Bulun, S.E., *Endometriosis*. N Engl J Med, 2009. **360**(3): p. 268-79.
2. Fourquet, J., et al., *Quantification of the impact of endometriosis symptoms on health-related quality of life and work productivity*. Fertil Steril, 2011. **96**(1): p. 107-12.
3. Fourquet, J., et al., *Patients' report on how endometriosis affects health, work, and daily life*. Fertil Steril, 2010. **93**(7): p. 2424-8.
4. Giudice, L.C. and L.C. Kao, *Endometriosis*. Lancet, 2004. **364**(9447): p. 1789-99.
5. Esfandiari, N., Z. Nazemian, and R.F. Casper, *Three-dimensional culture of endometrial cells: an in vitro model of endometriosis*. Am J Reprod Immunol, 2008. **60**(4): p. 283-9.
6. Guo, S.W., *Epigenetics of endometriosis*. Mol Hum Reprod, 2009. **15**(10): p. 587-607.
7. Martin, C. and Y. Zhang, *The diverse functions of histone lysine methylation*. Nat Rev Mol Cell Biol, 2005. **6**(11): p. 838-49.
8. Vaissiere, T., C. Sawan, and Z. Herceg, *Epigenetic interplay between histone modifications and DNA methylation in gene silencing*. Mutat Res, 2008. **659**(1-2): p. 40-8.
9. Monteiro, J.B., et al., *Endometriosis is characterized by a distinct pattern of histone 3 and histone 4 lysine modifications*. Reprod Sci, 2014. **21**(3): p. 305-18.
10. Colon-Caraballo, M., J.B. Monteiro, and I. Flores, *H3K27me3 is an Epigenetic Mark of Relevance in Endometriosis*. Reprod Sci, 2015. **22**(9): p. 1134-42.
11. Liu, X., Q. Zhang, and S.W. Guo, *Histological and Immunohistochemical Characterization of the Similarity and Difference Between Ovarian Endometriomas and Deep Infiltrating Endometriosis*. Reprod Sci, 2017: p. 1933719117718275.
12. Wu, Y. and S.W. Guo, *Inhibition of proliferation of endometrial stromal cells by trichostatin A, RU486, CDB-2914, N-acetylcysteine, and ICI 182780*. Gynecol Obstet Invest, 2006. **62**(4): p. 193-205.
13. Wu, Y. and S.W. Guo, *Suppression of IL-1beta-induced COX-2 expression by trichostatin A (TSA) in human endometrial stromal cells*. Eur J Obstet Gynecol Reprod Biol, 2007. **135**(1): p. 88-93.
14. Wu, Y., A. Starzinski-Powitz, and S.W. Guo, *Trichostatin A, a histone deacetylase inhibitor, attenuates invasiveness and reactivates E-cadherin expression in immortalized endometriotic cells*. Reprod Sci, 2007. **14**(4): p. 374-82.
15. Li, Y., et al., *Progesterone Alleviates Endometriosis via Inhibition of Uterine Cell Proliferation, Inflammation and Angiogenesis in an Immunocompetent Mouse Model*. PLoS One, 2016. **11**(10): p. e0165347.
16. Lu, Y., et al., *Trichostatin A, a histone deacetylase inhibitor, reduces lesion growth and hyperalgesia in experimentally induced endometriosis in mice*. Hum Reprod, 2010. **25**(4): p. 1014-25.

17. Mund, C. and F. Lyko, *Epigenetic cancer therapy: Proof of concept and remaining challenges*. *Bioessays*, 2010. **32**(11): p. 949-57.
18. Morera, L., M. Lubbert, and M. Jung, *Targeting histone methyltransferases and demethylases in clinical trials for cancer therapy*. *Clin Epigenetics*, 2016. **8**: p. 57.
19. Copeland, R.A., M.E. Solomon, and V.M. Richon, *Protein methyltransferases as a target class for drug discovery*. *Nat Rev Drug Discov*, 2009. **8**(9): p. 724-32.
20. Varier, R.A. and H.T. Timmers, *Histone lysine methylation and demethylation pathways in cancer*. *Biochim Biophys Acta*, 2011. **1815**(1): p. 75-89.
21. Margueron, R. and D. Reinberg, *The Polycomb complex PRC2 and its mark in life*. *Nature*, 2011. **469**(7330): p. 343-9.
22. Verma, S.K., et al., *Identification of Potent, Selective, Cell-Active Inhibitors of the Histone Lysine Methyltransferase EZH2*. *ACS Med Chem Lett*, 2012. **3**(12): p. 1091-6.
23. Amatangelo, M.D., et al., *Three-dimensional culture sensitizes epithelial ovarian cancer cells to EZH2 methyltransferase inhibition*. *Cell Cycle*, 2013. **12**(13): p. 2113-9.
24. Ding, M., et al., *The polycomb group protein enhancer of zeste 2 is a novel therapeutic target for cervical cancer*. *Clin Exp Pharmacol Physiol*, 2015. **42**(5): p. 458-64.
25. Liu, T.P., et al., *S-Adenosyl-L-methionine-competitive inhibitors of the histone methyltransferase EZH2 induce autophagy and enhance drug sensitivity in cancer cells*. *Anticancer Drugs*, 2015. **26**(2): p. 139-47.
26. Sato, T., et al., *Transcriptional Selectivity of Epigenetic Therapy in Cancer*. *Cancer Res*, 2017. **77**(2): p. 470-481.
27. Sun, F., et al., *Combinatorial pharmacologic approaches target EZH2-mediated gene repression in breast cancer cells*. *Mol Cancer Ther*, 2009. **8**(12): p. 3191-202.
28. Colon-Diaz, M., et al., *HDAC1 and HDAC2 are Differentially Expressed in Endometriosis*. *Reproductive sciences*, 2012.
29. Ruiz, A., et al., *Basal and steroid hormone-regulated expression of CXCR4 in human endometrium and endometriosis*. *Reproductive sciences*, 2010. **17**(10): p. 894-903.
30. Bulun, S.E., *Endometriosis*. *The New England journal of medicine*, 2009. **360**(3): p. 268-79.
31. Korch, C., et al., *DNA profiling analysis of endometrial and ovarian cell lines reveals misidentification, redundancy and contamination*. *Gynecol Oncol*, 2012. **127**(1): p. 241-8.
32. Torres-Reveron, A., et al., *Endometriosis Is Associated With a Shift in MU Opioid and NMDA Receptor Expression in the Brain Periaqueductal Gray*. *Reprod Sci*, 2016. **23**(9): p. 1158-67.
33. Geback, T., et al., *TScratch: a novel and simple software tool for automated analysis of monolayer wound healing assays*. *Biotechniques*, 2009. **46**(4): p. 265-74.

34. Attia, G.R., et al., *Progesterone receptor isoform A but not B is expressed in endometriosis*. The Journal of clinical endocrinology and metabolism, 2000. **85**(8): p. 2897-902.
35. Bulun, S.E., et al., *Estrogen receptor-beta, estrogen receptor-alpha, and progesterone resistance in endometriosis*. Seminars in reproductive medicine, 2010. **28**(1): p. 36-43.
36. Matsuzaki, S., et al., *Impaired down-regulation of E-cadherin and beta-catenin protein expression in endometrial epithelial cells in the mid-secretory endometrium of infertile patients with endometriosis*. The Journal of clinical endocrinology and metabolism, 2010. **95**(7): p. 3437-45.
37. Bulun, S.E., et al., *Steroidogenic factor-1 and endometriosis*. Molecular and cellular endocrinology, 2009. **300**(1-2): p. 104-8.
38. Grzenda, A., et al., *Functional characterization of EZH2beta reveals the increased complexity of EZH2 isoforms involved in the regulation of mammalian gene expression*. Epigenetics Chromatin, 2013. **6**(1): p. 3.
39. Zhang, Q., et al., *Enhancer of Zeste homolog 2 (EZH2) induces epithelial-mesenchymal transition in endometriosis*. Sci Rep, 2017. **7**(1): p. 6804.
40. Guo, S.W., *The endometrial epigenome and its response to steroid hormones*. Mol Cell Endocrinol, 2012. **358**(2): p. 185-96.
41. Meyer, J.L., et al., *DNA methylation patterns of steroid receptor genes ESR1, ESR2 and PGR in deep endometriosis compromising the rectum*. Int J Mol Med, 2014. **33**(4): p. 897-904.
42. Xu C, H.Z., Zhan P, Zhao W, Chang C, Zhou J, Hu H, Zhang Y, Yao X, Yu L, and Yan J. , *EZH2 regulates cancer cell migration through repressing TIMP-3 in non small cell lung cancer*. Med Oncol, 2013 Dec. **30**(4).
43. Chinaranagari S, S.P., and Chaudhary J. , *EZH2 dependent H3K27me3 is involved in epigenetic silencing of ID4 in prostate cancer*. Oncotarget, 2014 July 25.
44. Tan D, T.S., Zhang J, Tang P, Huang J, Zhou W, and Wu S., *Histone Trimethylation of the p53gene by expression of a constitutively active prolactin receptor in prostate cancer cells*. Chinese Journal of Physiology, 2013. **56**(5): p. 282-290.
45. Lu C, H.H., Mangala LS, Ali-Fehmi R, Newton CS, Ozbun L, et al., *Regulation of tumor angiogenesis by EZH2*. Cancer Cell 2010 August 9. **18**(2): p. 185-97.
46. Cao Q, Y.J., Dhanasekaran SM, Kim JH, Mani RS, Tomlins SA, et al. , *Repression of E-cadherin by the Polycomb Group Protein EZH2 in Cancer*. Oncogene, 2008 Dec 11. **27**(58): p. 7274-84.
47. Liu L, X.Z., Zhong L, Wang H, Jiang S, Long Q, Xu J, and Guo J., *EZH2 promotes tumor cell migration and invasion via epigenetic repression of E-cadherin in renal cell carcinoma*. BJU International, 2014 Feb 25.
48. Xu, C., et al., *EZH2 regulates cancer cell migration through repressing TIMP-3 in non-small cell lung cancer*. Med Oncol, 2013. **30**(4): p. 713.

49. Shin, Y.J. and J.H. Kim, *The role of EZH2 in the regulation of the activity of matrix metalloproteinases in prostate cancer cells*. PLoS One, 2012. **7**(1): p. e30393.
50. Purkait, S., et al., *EZH2 expression in gliomas: Correlation with CDKN2A gene deletion/ p16 loss and MIB-1 proliferation index*. Neuropathology, 2015. **35**(5): p. 421-31.
51. Jie, B., et al., *Enhancer of zeste homolog 2 depletion induces cellular senescence via histone demethylation along the INK4/ARF locus*. Int J Biochem Cell Biol, 2015. **65**: p. 104-12.
52. Bai, J., et al., *Inhibiting enhancer of zeste homolog 2 promotes cellular senescence in gastric cancer cells SGC-7901 by activation of p21 and p16*. DNA Cell Biol, 2014. **33**(6): p. 337-44.
53. Kikuchi, J., et al., *Epigenetic therapy with 3-deazaneplanocin A, an inhibitor of the histone methyltransferase EZH2, inhibits growth of non-small cell lung cancer cells*. Lung cancer, 2012. **78**(2): p. 138-43.
54. Nakagawa, S., et al., *Epigenetic therapy with the histone methyltransferase EZH2 inhibitor 3-deazaneplanocin A inhibits the growth of cholangiocarcinoma cells*. Oncol Rep, 2014. **31**(2): p. 983-8.
55. Li, Z., et al., *The polycomb group protein EZH2 is a novel therapeutic target in tongue cancer*. Oncotarget, 2013. **4**(12): p. 2532-49.
56. Trenkmann, M., et al., *Expression and function of EZH2 in synovial fibroblasts: epigenetic repression of the Wnt inhibitor SFRP1 in rheumatoid arthritis*. Ann Rheum Dis, 2011. **70**(8): p. 1482-8.
57. Greathouse, K.L., et al., *Environmental estrogens differentially engage the histone methyltransferase EZH2 to increase risk of uterine tumorigenesis*. Mol Cancer Res, 2012. **10**(4): p. 546-57.

Figure Legends

Figure 1

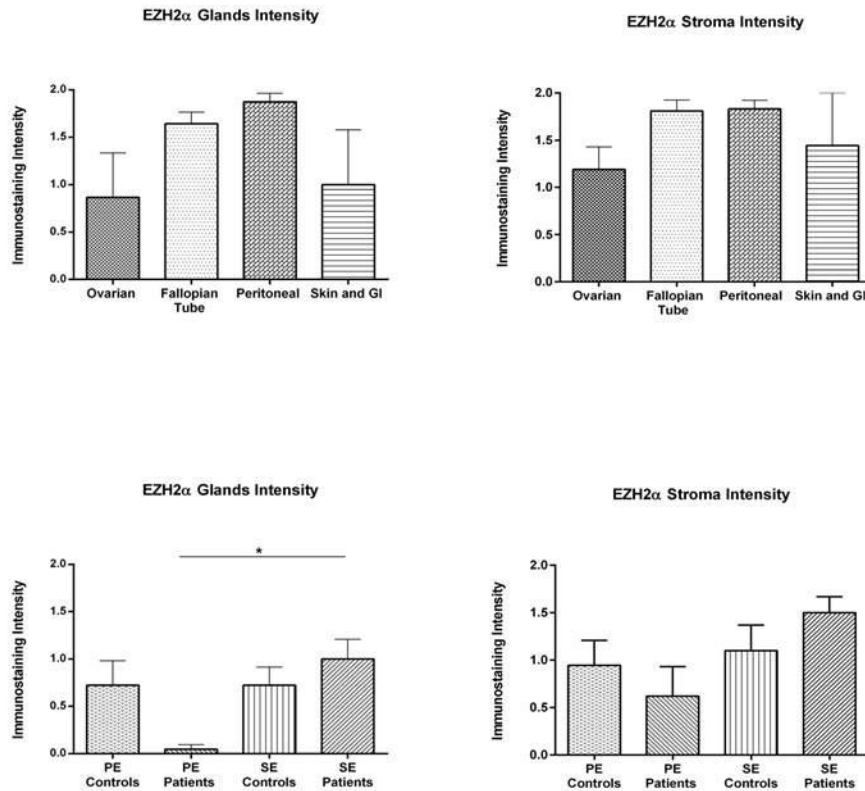


Figure 1: Immunostaining intensity for EZH2α in endometriotic lesions and endometrium from patients and controls. Immunostaining of EZH2α in glands and stroma was analyzed by three independent scorers using an intensity scale (2=strong, 1=weak, and 0=no staining). Immunostaining was reported as mean intensity ± SEM. No significant differences based on the immunostaining intensity for EZH2α was observed among the different lesions type neither in glands nor stroma. Significant higher intensity of EZH2α was observed in the glands of the secretory endometrium from patients compared to proliferative endometrium from patients (SE-Patients vs. PE Patients p=0.0254).

Figure 2

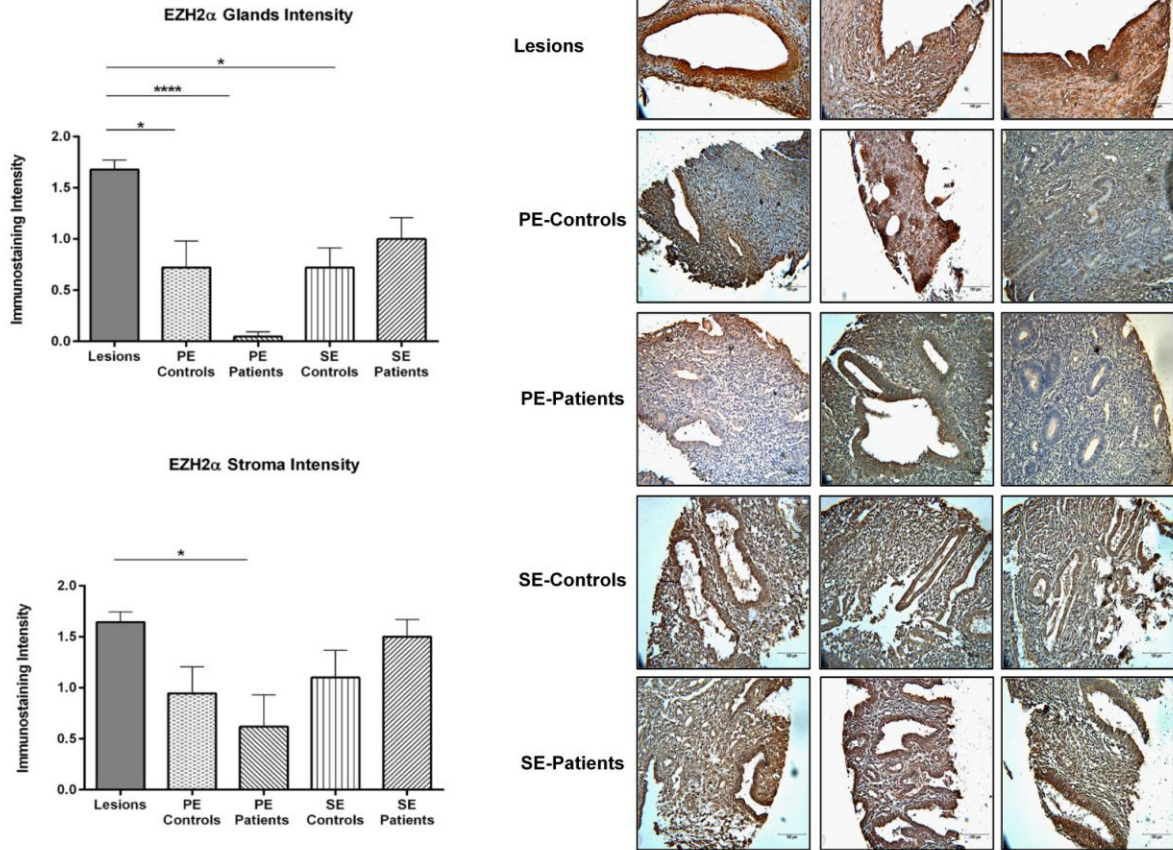


Figure 2: Immunostaining intensity for EZH2α in endometriotic lesions and endometrium from patients and controls. Immunostaining of EZH2α in glands and stroma was analyzed by three independent scorers using an intensity scale (2=strong, 1=weak, and 0=no staining). Immunostaining was reported as mean intensity \pm SEM. Significant higher intensity of EZH2α was observed in the glands and stroma of endometriotic lesions compared to proliferative endometrium (from patients and controls) and secretory endometrium (from patients) ($p < 0.05$). Representative pictures of EZH2α nuclear immunostaining in lesions and endometria from patients with endometriosis (PE-Patients) are shown to demonstrate specificity of the antibody and differential expression.

Figure 3

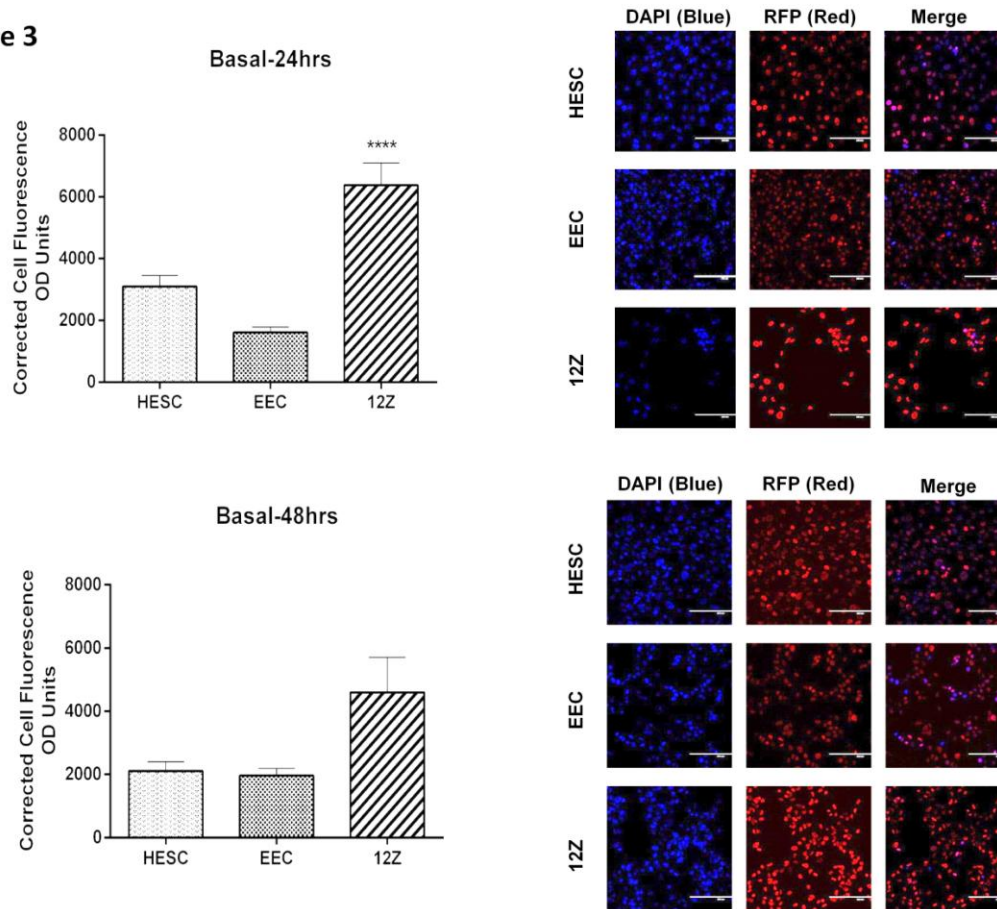


Figure 3: Basal Enrichment of H3K27me3 in Endometriotic Epithelial Cells (12Z), Non-Endometriotic Stromal Cells (HESC), and Non-Endometriotic Epithelial Cells (EEC). Fluorescent Intensity of

H3K27me3 was detected by IF using a specific antibody against H3K27me3. Immunofluorescence Intensity for H3K27me3 was measured at 24hrs and 48hrs using Image-J. H3K27me3 enrichment levels were determined using the CTCF formula. Kruskal-Wallis Test (Non-parametric ANOVA) was used for statistical analysis. Significance was set as $p < 0.05$. Representative pictures of DAPI (blue, which stain the nucleus), RFP (red, which stain H3K27me3 mark in the nucleus) and Merge (DAPI and RFP) are shown to demonstrate the specificity of the antibody.

Figure 4

12Z

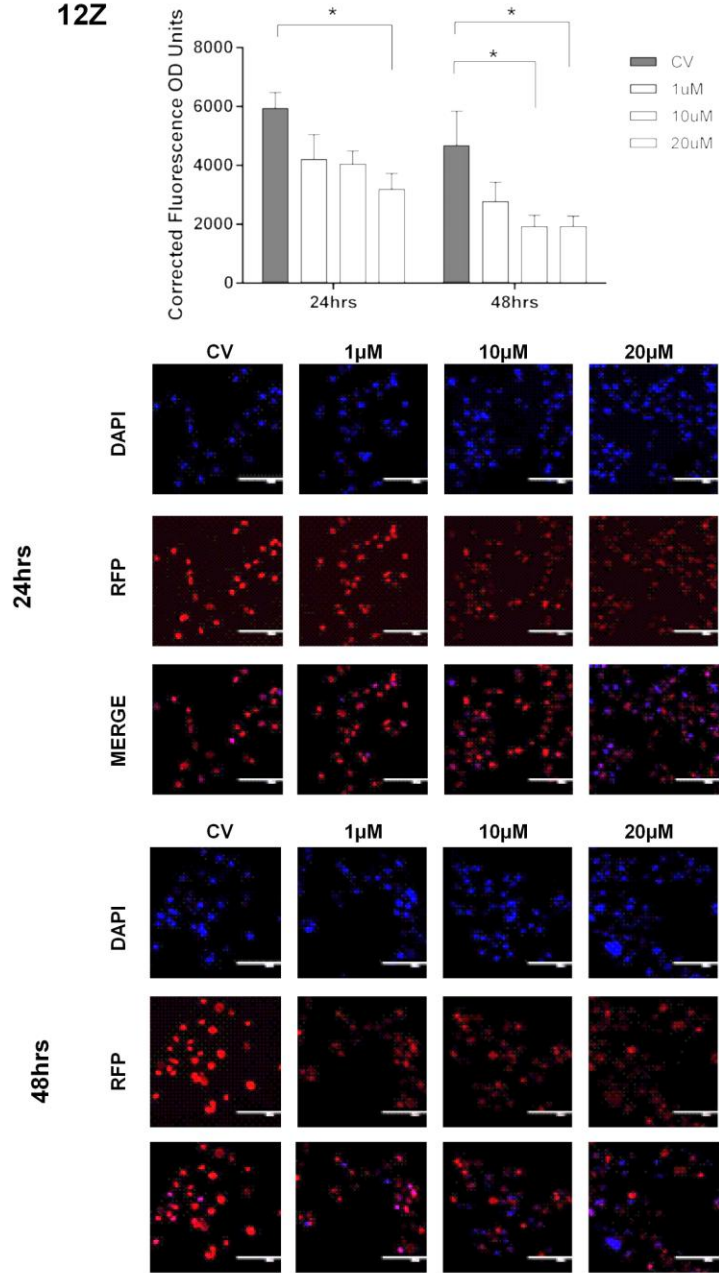


Figure 4: Effect of EZH2 Pharmacological Inhibition in the Enrichment of H3K27me3 in Endometriotic Epithelial Cells (12Z). Cells were treated with GSK343 (1 μ M, 10 μ M, and 20 μ M) for 24hrs and 48hrs, respectively. Fluorescent Intensity of H3K27me3 was detected by IF using a specific antibody against H3K27me3. Immunofluorescence Intensity for H3K27me3 was measured at 48hrs using Image J. H3K27me3 enrichment levels was determined using the CTCF formula. Low enrichment levels of H3K27me3 were detected when cells were treated with 20 μ M at 24hrs ($p < 0.05$ compared to CV) and 10 μ M and 20 μ M at 48hrs ($p < 0.05$ compared to CV). Two-way Anova Test followed by Tukey Post-hoc analysis was used for statistical analysis. Significance was set as $p < 0.05$. Representative pictures of DAPI (blue, which stain the nucleus), RFP (red, which stain H3K27me3 mark in the nucleus) and Merge (DAPI and RFP) are shown to demonstrate the specificity of the antibody and the efficacy of the treatment.

Figure 5

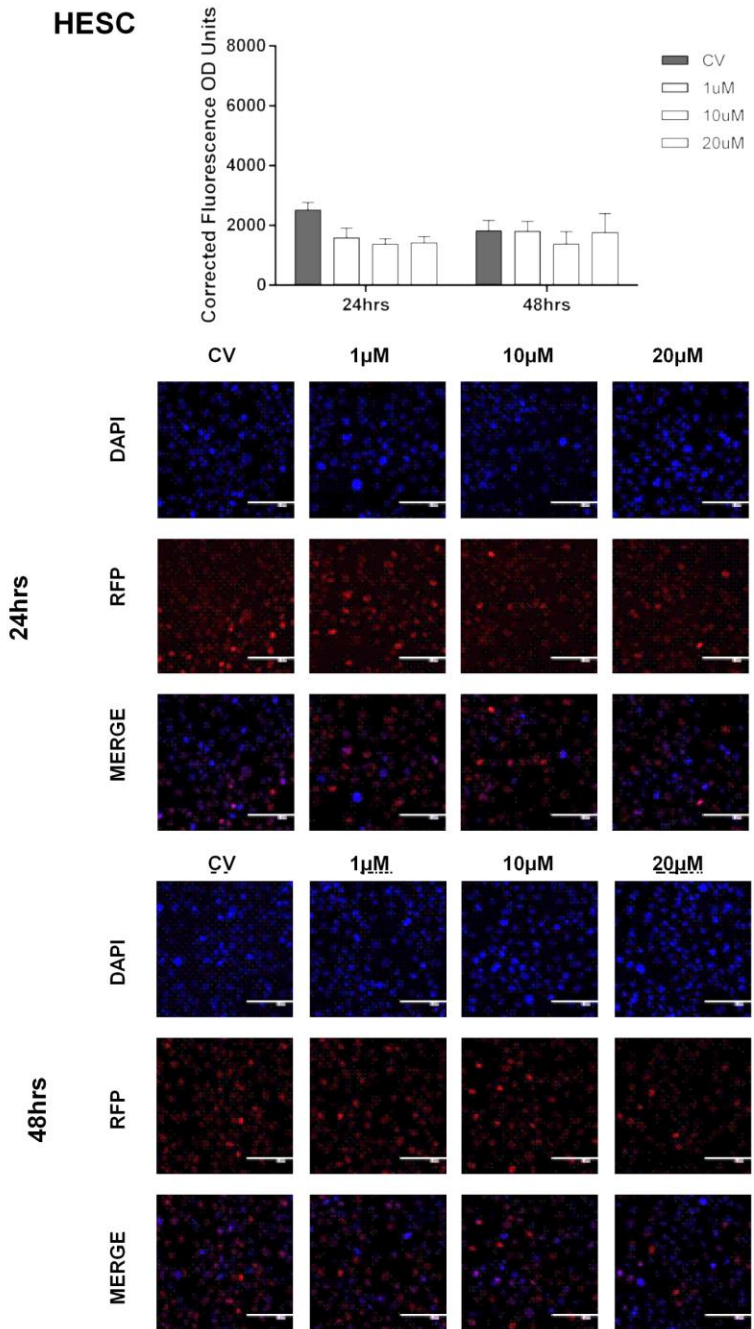


Figure 5: Effect of EZH2 Pharmacological Inhibition in the Enrichment of H3K27me3 in Non-

Endometriotic Stromal Cells (HESC) cells. Cells were treated with GSK343 (1 μ M, 10 μ M, and 20 μ M) for 24hrs and 48hrs, respectively. Fluorescent Intensity of H3K27me3 was detected by IF using a specific antibody against H3K27me3. Immunofluorescence Intensity for H3K27me3 was measured at 48hrs using Image J. H3K27me3 enrichment levels was determined using the CTCF formula. Low enrichment levels of H3K27me3 were detected when cells were treated with 20 μ M at 24hrs ($p < 0.05$ compared to CV) and 10 μ M and 20 μ M at 48hrs ($p < 0.05$ compared to CV). Two-way Anova Test followed by Tukey Post-hoc analysis was used for statistical analysis. Significance was set as $p < 0.05$. Representative pictures of DAPI (blue, which stain the nucleus), RFP (red, which stain H3K27me3 mark in the nucleus) and Merge (DAPI and RFP) are shown to demonstrate the specificity of the antibody and the efficacy of the treatment.

Figure 6

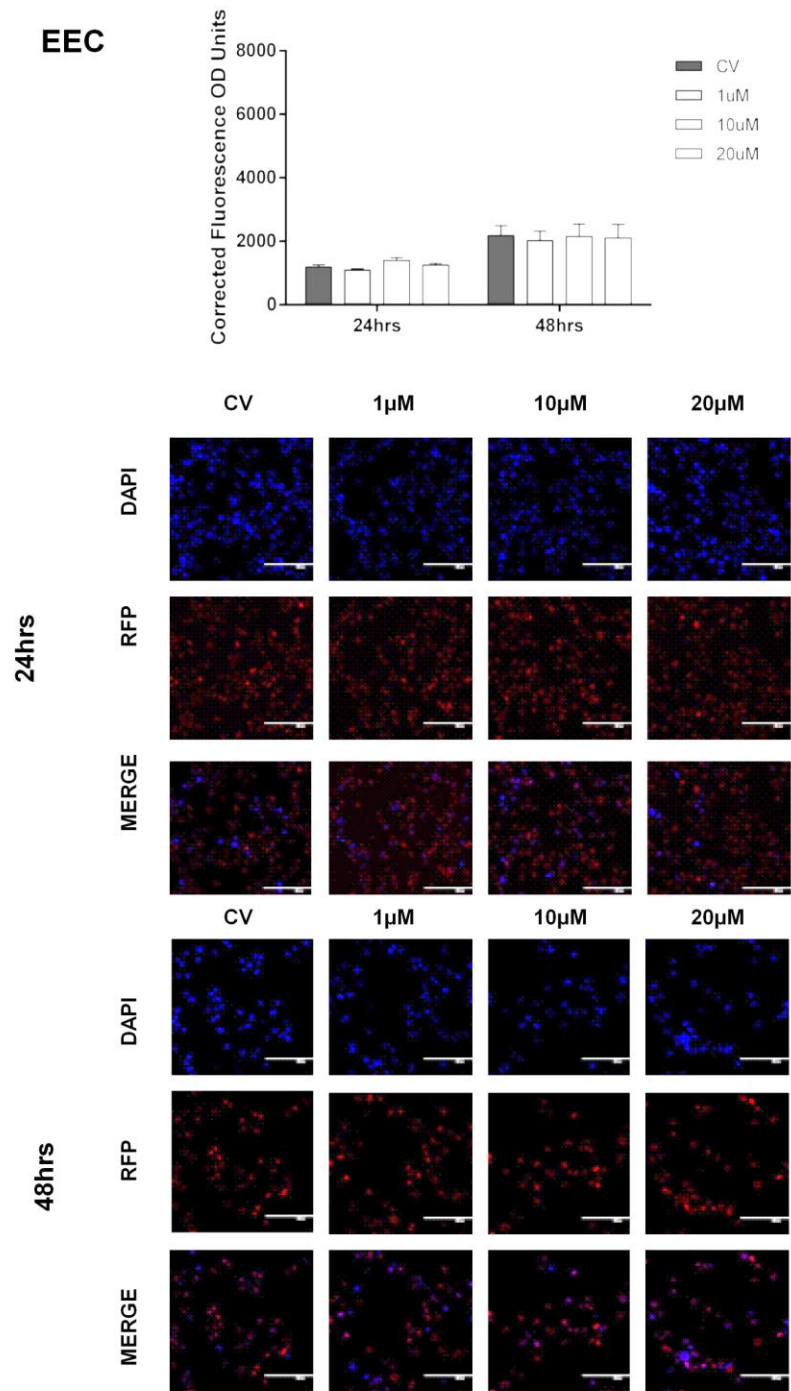


Figure 6: Effect of EZH2 Pharmacological Inhibition in the Enrichment of H3K27me3 in Non-

Endometriotic Epithelial Cells (EEC) cells. Cells were treated with GSK343 (1 μ M, 10 μ M, and 20 μ M) for 24hrs and 48hrs, respectively. Fluorescent Intensity of H3K27me3 was detected by IF using a specific antibody against H3K27me3. Immunofluorescence Intensity for H3K27me3 was measured at 48hrs using Image J. H3K27me3 enrichment levels was determined using the CTCF formula. Low enrichment levels of H3K27me3 were detected when cells were treated with 20 μ M at 24hrs ($p < 0.05$ compared to CV) and 10 μ M and 20 μ M at 48hrs ($p < 0.05$ compared to CV). Two-way Anova Test followed by Tukey Post-hoc analysis was used for statistical analysis. Significance was set as $p < 0.05$. Representative pictures of DAPI (blue, which stain the nucleus), RFP (red, which stain H3K27me3 mark in the nucleus) and Merge (DAPI and RFP) are shown to demonstrate the specificity of the antibody and the efficacy of the treatment.

Figure 7

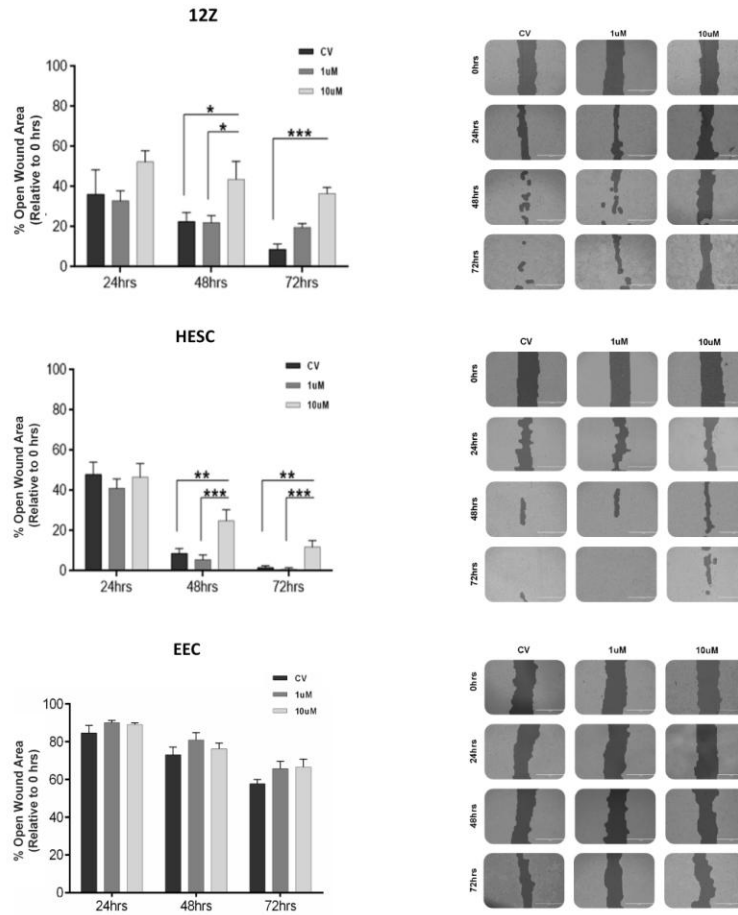


Figure 7: Effect of EZH2 Inhibition in the Migration Capacity of Human Endometriotic Epithelial Cells

(12Z) and Endometrial Cells Treated with GSK343. Different concentrations of GSK-343 (1 μ M and

10 μ M) were added to the cells for 72hrs. Data was normalized against 0hrs. Experiments were

conducted in duplicate (3 replicates per condition per plate). The % of open wound area of the cells

was determined using T-Scratch software. Two -way ANOVA followed by Tukey's multiple comparisons

test was conducted for statistical analysis. Significance was set as $p < 0.05$. Representative pictures of

the Migration Capacity of Human Endometriotic Epithelial Cells (12Z) treated with GSK343. The

pictures were taken at 0, 24, 48, and 72 hours using an inverted microscope (EVOS-FL). Pictures are

presented in the format in which the program (T-Scratch Software) denotes the open wound area of

the cells.

Figure 8

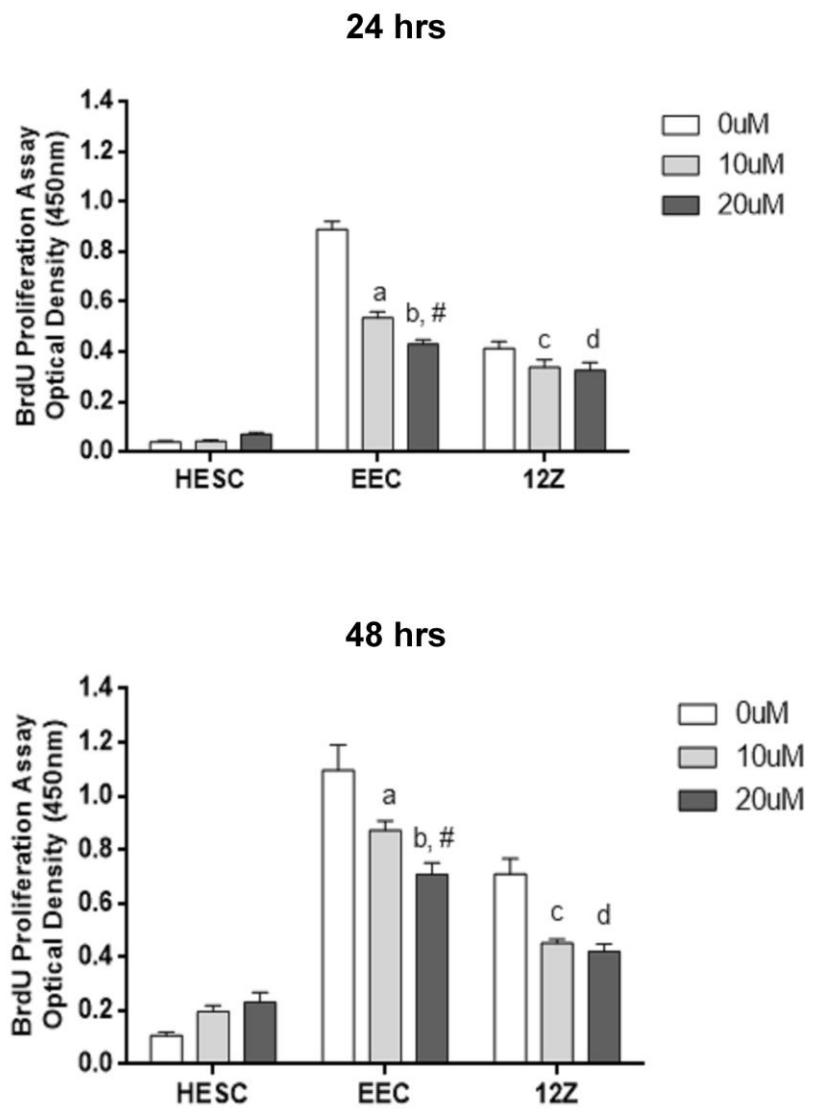
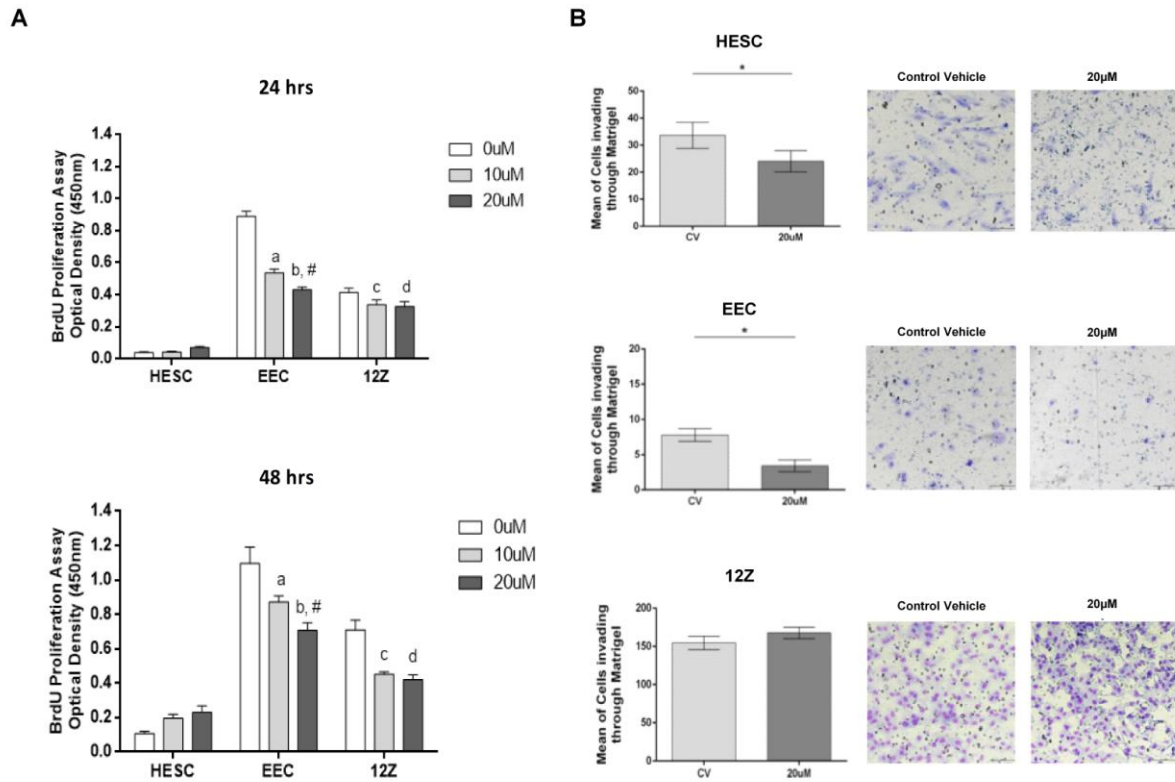


Figure 8:

A) Effect of EZH2 inhibitor, GSK343, in the proliferation rates of endometriotic and non-endometriotic cells. BrdU analysis was performed in the human endometrial stromal cells (HESC) and the human non-endometriotic (EEC) and endometriotic (12Z) epithelial cells treated with GSK343 for 24hrs and 48hrs. At 24hrs, the proliferative rate of EEC cells significantly decreased at 10uM (relative to 0uM; $p < 0.0001^a$) and 20uM (relative to 0uM; $p < 0.0001^b$ and relative to at 10uM $p = 0.005^{\#}$). For 12Z

cells, the proliferative rate significantly decreased at 20uM (relative to 0uM; $p < 0.05^d$) and a borderline significance decreased was observed at 10uM ($p = 0.0553^c$). At 48hrs, the proliferative rate of EEC cells significantly decreased at 10uM (relative to 0uM; $p = 0.0019^a$) and 20uM (relative to 0uM; $p < 0.0001^b$ and relative to at 10uM; $p < 0.05^#$). For 12Z cells, the proliferative rate significantly decreased at 10uM (relative to 0uM; $p = 0.0003^c$) and 20uM (relative to 0uM; $p < 0.0001^d$). Normalization was done by subtracting the blank (medium only). Experiments were performed in triplicate. Two-way ANOVA followed by Tukey's multiple comparisons test was conducted to determine statistical analysis. Significance was set as $p < 0.05$.

Figure 9



B) Effect of EZH2 inhibitor, GSK343, in the invasiveness of endometriotic (12Z) and non-endometriotic (HESC and EEC) cells. Matrigel assay was performed in the human endometrial stromal cells (HESC), non endometriotic epithelial cells (EEC) and endometriotic epithelial cells (12Z). Experiments were performed in triplicate (two technical replicates by each experiment). Wilcoxon test was conducted to determine statistical analysis. Significance was set as $p < 0.05$. Representative pictures of the Invasion Capacity of HESC, EEC, and 12Z cells treated with GSK343. The pictures were taken at the end of the experiment at 24 hours using a High Intensity LED Light Inverted Nikon Eclipse TS2R-FL microscope at 20X objective (Nikon, Melville, NY) with an adapted camera DS-Ri2.

Table 1

Table 1: Demographic Characteristics of Study Patients used for ChIP Analysis						
Pt ID	Diagnosis	Age	ASRM Stage	Tissue	Reg Cycle	Phase
658A	Endometriosis	45	2	Ovarian endometriosis	Yes	Proliferative
741A	Endometriosis	44	2	Endometrioma	Yes	Secretory
741B	Endometriosis	44	2	Ovarian endometriosis	Yes	Secretory
786	Endometriosis	25	1	Peritoneal Endometriosis	Yes	Unknown
837	Endometriosis	32	1	Ovarian endometriosis	Yes	Secretory
940	Endometriosis	28	2	Ovarian endometriosis	Yes	Proliferative
1008	Endometriosis	42	2	Ovarian endometriosis	Yes	Unknown
1025	Endometriosis	37	2	Endometrioma	Yes	Proliferative
1025A	Endometriosis	37	2	Right Ovarian endometriosis	Yes	Proliferative
1025B	Endometriosis	37	2	Left Ovarian endometriosis	Yes	Proliferative
1141	Endometriosis	28	2	Ovarian endometriosis	Yes	Proliferative
1260	Endometriosis	Unknown	Unknown	Peritoneal Endometriosis	Yes	Unknown
1263	Endometriosis	Unknown	Unknown	Ovarian endometriosis	Yes	Unknown
Pt ID	Diagnosis	Age	ASRM Stage	Tissue	Cycle Day	Phase
N014	Healthy Control	Unknown	N/A	Endometrium	5	Proliferative
N016	Healthy Control	Unknown	N/A	Endometrium	8	Proliferative
N018	Healthy Control	Unknown	N/A	Endometrium	8	Proliferative
N020	Healthy Control	Unknown	N/A	Endometrium	6	Proliferative
N024	Healthy Control	Unknown	N/A	Endometrium	5	Proliferative
N027	Healthy Control	Unknown	N/A	Endometrium	6	Proliferative
N009	Healthy Control	Unknown	N/A	Endometrium	23	Mid Secretory
N015	Healthy Control	Unknown	N/A	Endometrium	23	Mid Secretory
N030	Healthy Control	Unknown	N/A	Endometrium	21	Mid Secretory
N032	Healthy Control	Unknown	N/A	Endometrium	Unknown	Mid Secretory
N037	Healthy Control	Unknown	N/A	Endometrium	22	Mid Secretory
N045	Healthy Control	Unknown	N/A	Endometrium	Unknown	Mid Secretory

Table 2

Table 2: Primers of Candidate Genes in Endometriosis					
Gene Name	Primer Name	Sequence	Primer Name	Sequence	Product Size (bp)
CDH1	CDH1-R	GAGTCACCCGGTTCATCTA	CDH1-F	GGTGTGGGAGTGCAATTTCT	229
ESR1	ESR-1 R	GAAAGCCTTGCCACTCTGAC	ESR-1 F	TCTATGGGATCCAACCTCCA	212
HOXA10	HOXA10-R	CTGGCCCATCTTCCAAGTAA	HOXA10-F	GCTAAGCCGTAGATGCTTGC	156
HOX9	HOX9-R	CCCATCGATCCCAGTAAGTG	HOX9-F	CGTCCAAACACCAACTTCT	161
NR5A1	NR5A1-R	CTTACCCACTCCACGCTGT	NR5A1-F	GCAGTCCAGCTCGAGTCTTC	247
PGR_MR	PGR_MR-R	ACACCTTGCCTGAAGTTTCG	PGR_MR-F	CTGGGGGACTAGAACTGCTG	186

Table 3: H3K27me3 enrichment in promoter regions of candidate genes

Gene	Tissue Type	10-Fold Enrichment or more	Less than 10-Fold Enrichment	Missing (No Ct Value)	p-value*
PGR	Endometriotic Lesions	4/13 (31%)	9/13	0/13	1.0
	Healthy Controls	4/12	8/12	0/12	
HOXA10	Endometriotic Lesions	3/13	9/13	1/13	1.0
	Healthy Controls	3/12	9/12	0/12	
HOXA9	Endometriotic Lesions	2/13	11/13	0/13	1.0
	Healthy Controls	1/12	11/12	0/12	
CDH1	Endometriotic Lesions	6/13 (46%)	7/13	0/13	0.03
	Healthy Controls	11/12	1/12	0/12	
ESR1	Endometriotic Lesions	9/13 (69%)	4/13	0/13	0.04
	Healthy Controls	3/12	9/12	0/12	
NR5A1 (SF-1)	Endometriotic Lesions	3/13	10/13	0/13	1.0
	Healthy Controls	3/12	9/12	0/12	

* Fischer's exact test to determine associations between groups (cases and controls) and H3K27me3 enrichment. Statistical significance was set as p<0.05